

# Mechanical Design of a Biomimetic Compliant Lower Limb Exoskeleton (BioComEx)

Ozgur Baser, Hasbi Kizilhan and Ergin Kilic

Department of Mechanical Engineering

Suleyman Demirel University

Isparta, Turkey

e-mails: {ozgurbaser, hasbikizilhan, erginkilic}@sdu.edu.tr

**Abstract**— Exoskeleton robots are wearable electromechanical structures interacting with human limbs. They are used for extending or replacing human performance in power augmentation and rehabilitation applications. The neuromuscular system of the human body provides flexible and stable movement with minimum energy consumption by means of the compliant actuation of human joints. Similar to human body, compliant actuation can be used to maximize the performance in exoskeleton robots. In the present study, we designed a new biomimetic compliant lower limb exoskeleton robot (BioComEx). Firstly, the current exoskeleton robot designs and biomechanics of the human body joints are reviewed. Then, according to the inferences of human joint biomechanics review, ankle joint is designed as variable stiffness actuator; knee and hip joints are designed as series elastic actuators. Kinetostatic analysis of these joint mechanisms is conducted, and finally the design details of each joint and complete exoskeleton structure adapted to a human dummy model are explained.

**Keywords** - Lower Limb Exoskeleton, Variable Stiffness Actuator, Series Elastic Actuator

## I. INTRODUCTION

The exoskeleton robots are electromechanical structures worn by the user and interacting with human limbs. They are used as rehabilitation devices for injured joints because of the neurological disorders or power augmentation assistants for military applications.

A considerable increase in the implementations of exoskeletons has been seen in the last few years and thus, various designs are introduced for power augmentation and rehabilitation. Firstly, for power augmentations; Kanazawa Institute of Technology developed the full body exoskeleton robots. The robot is used to augment the nurse's power to take care of the patient [1]. Then, University of Tsukuba has developed different version of Robot Suit Hal to physically support a user's daily activities and heavy work [2]. Another consideration is the BLEEX, a lower limb exoskeleton from Berkeley University, has been designed to augment the human limb so that the wearer is able to carry heavy load easily over various terrains [3]. The second purpose of the exoskeleton robots is the rehabilitation. Therefore, various exoskeleton robots have been developed for rehabilitation applications. Those are implemented in either the lower limb for gait rehabilitation or the upper limb for regain the arm joints functions. The treadmill gait trainer is one implementation of gait rehabilitation. There are some robotic systems for treadmill gait training in the literature. The LOKOMAT exoskeleton is an example of the early treadmill gait trainer. It consists of a robotic gait orthosis and an advanced body weight support system combined with a treadmill. It uses computer

controlled actuators which are integrated in the gait orthosis at each hip and knee joint. The actuators are precisely synchronized with the speed of the treadmill to assure a precise match between the speed of the gait orthosis and the treadmill [4]. In addition, there are many other treadmill gait trainer exoskeletons such as LOPES [5], LokoHelp [6], ReoAmbulator [7], and ALEX [8]. LOPES can move in parallel with the legs of a person walking on a treadmill, it has pelvis height flexibly connected to the fixed world. LokoHelp is another electromechanical device developed for improving gait after brain injury. The device is placed to the middle of the treadmill surface parallel to the walking direction and fixed to the front of the treadmill with a single clamp. It also provides a body weight support system for the patient [6]. Reo-Ambulator is a body-weight-supported treadmill robotic system. Robotic arms are strapped to the patient's legs at the thigh and ankle driving them through a stepping pattern. A single-blind randomized clinical trial to assess its effectiveness in stroke patients is currently underway [7]. ALEX is designed as body-weight-supported treadmill robotic system. It is powered leg orthosis with linear actuators at the hip and knee joints and with a force-field controller developed to provide assistance to the patient by using the assist-as-needed approach [8].

This study introduces the design of a new biomimetic compliant lower limb exoskeleton robot. This robot is called as BioComEx in this paper. Firstly, the biomechanics of the human body lower limb joints are reviewed. The kinetostatic analysis for the joints of BioComEx is presented in the next section. Then, its mechanical design is described in detail. Finally, the conclusion and future works are discussed.

## II. HUMAN BODY LOWER LIMB JOINTS BIOMECHANICS

Exoskeleton robots that interact with human limbs should mimic the biomechanics behaviors of human body limbs for compliance. Therefore, understanding biological behavior of human lower body joints is critical for designing exoskeleton and evaluating human locomotion. Because of this, the biomechanical behavior of lower joints has been characterized by using some bio-mechanic studies in this section. The compliance term for the lower joints can be examined as the concept of quasi-stiffness or dynamic stiffness. The quasi-stiffness term is usually reserved for ankle, knee and hip joints. It is defined as the slope of the best linear fit on the moment-angle graph of a joint over a whole gait or specific phase of a gait [9-10]. According to this, the phases of ankle, knee and hip joints during gait cycle and their stiffness are explained in this section.

The human gait cycle begins primarily when one foot initially touches the ground and ends when the same foot

touches the ground again after completing stance and swing phases. Firstly, the phases and the quasi-stiffness of the ankle are defined during the gait cycle. The ankle undergoes stance and swing phases during one gait cycle. The body is pushed forward in the stance phase [11]. The stance phase can be divided into three sub-phases during this progression period including dorsi-flexion, dual-flexion and plantar-flexion phases. The quasi-stiffness of the ankle is defined for stance phase of walking because the ankle is loaded in this phase. Fig.1 shows the human ankle's moment-angle relative curve for a representative subject walking at 1.75 m/s. As shown in the figure, dorsi-flexion (b-c), dual-flexion (c-d) and plantar-flexion (d-e) sub-phases are represented by separate line fitting on the moment-angle curve [12]. This means that the ankle neuro-muscular system adjusts the joint stiffness to different stiffness values for different sub-phases. So, it tells that ankle's stiffness is constantly changed during the gait cycle. Therefore, to ensure energy efficiency and flexible movement, variable stiffness actuator designs need to be used at the ankle joint of the exoskeletons [13].

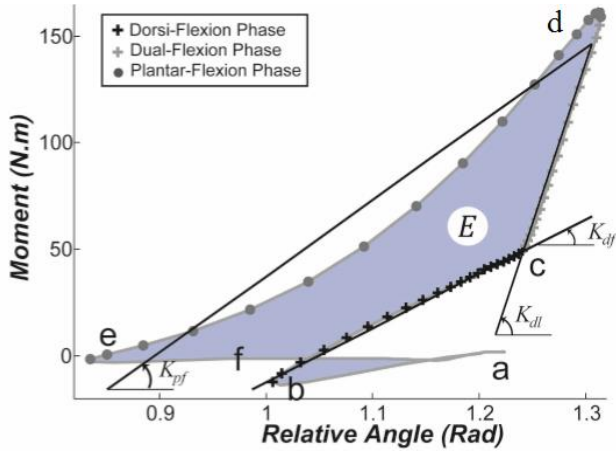


Figure 1. Human ankle's moment-angle relative curve [13]

The knee joint also undergoes stance and swing phases during gait cycle similar to ankle joint. The stance phase can be divided into two sub-phases including a weight acceptance phase and a stance termination phase. In this study, the weight acceptance sub-phase is centered for the quasi-stiffness of the knee joint because a substantial moment is applied to support the body weight. In this phase, the knee joint undergoes a flexion movement (a-b) and an extension movement (b-c) while supporting body weight. The human knee's moment-angle relative curve for a representative subject walking at 1.25 m/s is shown in Fig. 2. As shown in the figure, the quasi-stiffness of the knee is calculated based on the slope of the best fit line to the moment-angle curve (a-b) for the flexion and (b-d) for extension movement of the weight acceptance phase (a-d) [14]. It is understood from the figure that the stiffness of the flexion and extension are very close linear lines. Therefore, one stiffness value can be taken for the knee stiffness instead of taking two different stiffness values as flexion and extension. Thus, series elastic actuator design, having a single stiffness, can be used for the knee joints of the exoskeletons [14].

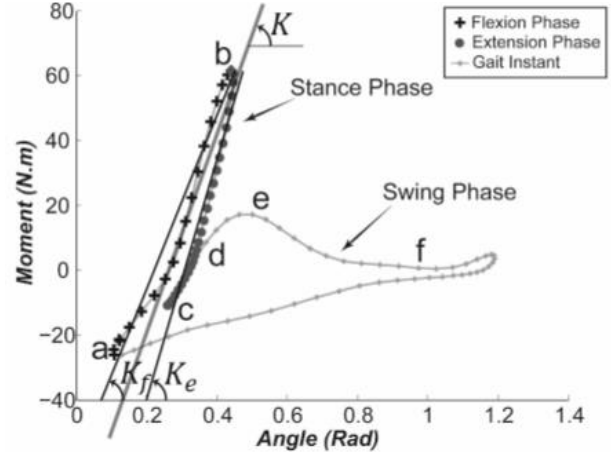


Figure 2. Human knee's moment-angle relative curve [14]

Hip joint also consists of stance and swing phases during the gait cycle just as ankle and knee joints. The stance phase of the hip joint can be divided into initial, mid and terminal sub-phases. Fig.3 shows the hip joint moment-angle graph for a representative subject walking at 2.17 m/s of walking velocity. As shown in the figure, the quasi-stiffness of the hip is characterized in the resilient loading phase of the gait (Fig. 3, c-e), where the hip exhibits a nearly linear extension stage (c-d) and flexion stage (d-e) [15]. Similar to the knee joint, the lines of the flexion and extension are very close linear lines. Therefore, one stiffness value can be taken for the hip stiffness instead of taking two different stiffness values as flexion and extension. Thus, again series elastic actuator design, having a single stiffness, can be used for the hip joints of the exoskeletons [15].

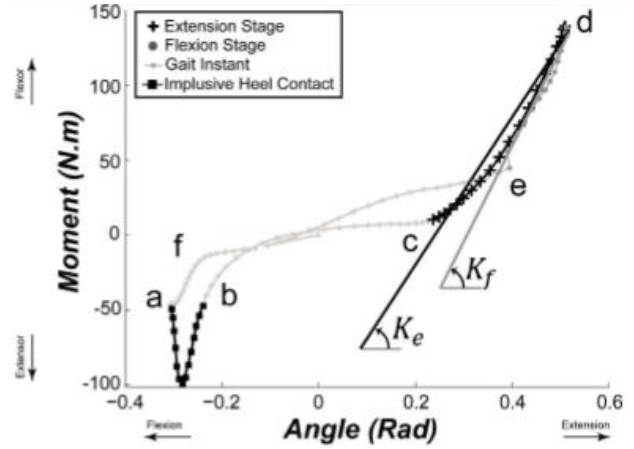


Figure 3. Human hip's moment-angle relative curve [15]

### III. KINETOSTATIC ANALYSIS OF EXOSKELETON ROBOT JOINTS

In this section, the kinetostatic analysis of the BioComEx's joint actuators is presented. According to this analysis, power requirement of the actuators can be calculated and appropriate

motor selection can be made depending upon the derived equations.

Firstly, the equations of the ankle joint are given. In our previous study [16], we compared the performances of the different variable stiffness actuator mechanisms (Controllable transmission ratio type, Antagonistic type and Pre-tension type variable stiffness actuators) for the ankle joint. This previous study showed that the controllable transmission ratio type actuator is better than the others in terms of power requirement and energy consumption. Therefore, we used the working principle of the controllable transmission ratio type variable stiffness actuator mechanism in the ankle joint. Fig. 4 shows the schematic view of the ankle actuator of BioComEx. As shown in the figure, first motor (M1) controls the equilibrium position of the ankle joint while the second motor (M2) performs stiffness adjustment. The stiffness of this type of actuator design is adjusted by changing the transmission ratio between the spring and output link. In the design presented in this paper, the pivot point and spring position are constant and the position of the force arm is controlled, and thus the stiffness of the actuator can be tuned to a desired value. Linear springs are used in this actuator as elastic element because the equivalent output stiffness of the variable stiffness actuator is expected to be almost linear.

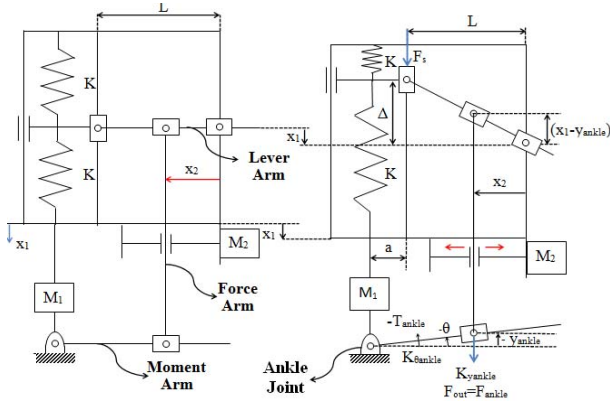


Figure 4. Schematic view of the variable stiffness actuator mechanism used in the ankle of BioComEx

As shown in the figure,  $x_1$  represents the equilibrium position of the whole mechanism and is controlled by first motor (M1). Eq.(1) can be used to calculate the required position of the first motor for providing ankle joint moment.

$$x_1 = (a + L - x_2) \tan(\theta_{ank}) + \frac{T_{ank} x_2^2}{2L^2(a+L-x_2)K} \quad (1)$$

In this design,  $x_2$  represents the position of the output link to be controlled by second motor for the ankle joint stiffness adjustment and is calculated by using Eq.(2).

$$x_2 = \frac{(a+L)L}{L + \cos(\theta_{ank}) \sqrt{\frac{K\theta_{ank}}{2K}}} \quad (2)$$

In Eq.(2),  $\theta_{ank}$ ,  $K_{\theta_{ank}}$  and  $K$  represent the ankle joint, the desired rotational stiffness of the ankle joint and the spring stiffness used in the mechanism, respectively.

The forces applied by the first and the second motor can be expressed as Eq.(3) and (4).

$$F_{m1} = -2K \frac{L^2}{x_2^2} [(a + L - x_2) \tan(\theta_{ank})] \quad (3)$$

$$F_{m2} = F_{ank} [\cos \alpha * \sin \alpha + \cos(\theta_{ank}) \sin(\theta_{ank})] \quad (4)$$

$$\text{where } \alpha = \arctan \left[ \frac{x_1 - (a+L-x_2) \tan(\theta_{ank})}{x_2} \right]$$

Finally, the power requirement (P) can be calculated by using Eq. (5).

$$P = P_{m1} + P_{m2} = F_{m1} \dot{x}_1 + F_{m2} \dot{x}_2 \quad (5)$$

As mentioned in the previous section, the knee and hip joints can be designed as series elastic actuator, since the stiffness of the joints is nearly constant during gait cycle. Fig. 5 shows the schematic view of the series elastic actuator mechanism used for hip and knee joints. The motor (M) moves the whole mechanism, and hence adjust the joint equilibrium position of the joint via force and moment arms.

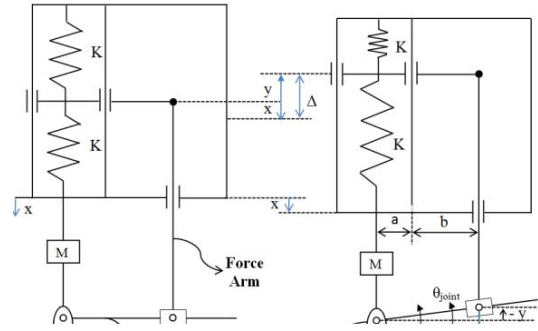


Figure 5. Schematic view of the series elastic actuator mechanism used in the knee and hip of BioComEx

Similar to the variable stiffness actuator, the force and displacement of the motor were derived in Eqs. (6) and (7).

$$F_m = \frac{T_{joint}}{(a+b)} \quad (6)$$

$$x = \frac{T_{joint}}{2(a+b)K} - (a+b) \tan(\theta_{joint}) \quad (7)$$

These two equations can be used for both knee and hip joints since their mechanism are the same.  $T_{joint}$  and  $\theta_{joint}$  represent the joint moment and joint position for the knee and hip joints. Besides,  $K$  is the spring stiffness used in the mechanism and the other symbols ( $a$  and  $b$ ) are the geometric parameters of the mechanism. After the force and displacement calculations, the power requirement of the joint mechanisms can be calculated as similar to Eq. (5).

Firstly, we need joint torque and joint position variations for one walking cycle to calculate the power requirement. The data provided by Bovi et al. [17] study on bio-mechanics have been used in this study. According to these data, lower limbs' joint position angle and moment values of an optimum walking speed ( $0.8 \leq \text{walking speed/height} \leq 1$ ) of an average adult, with 80 kg weight, are shown in Fig. 6.

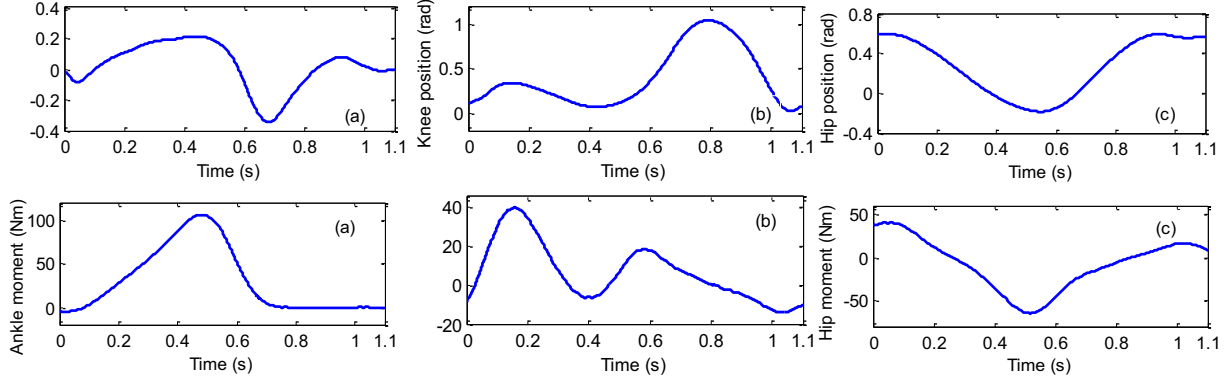


Figure 6. The variation of the angle position and moment during one gait cycle for (a) ankle, (b) knee and (c) hip joints

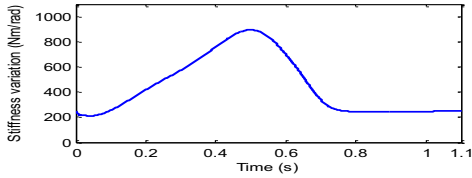


Figure 7. Variation of ankle joint stiffness

By using the variation of joint moment, joint position and ankle stiffness during one walking gait

In addition to the joint position and joint moments, the stiffness variation of the angle joint ( $K_{\theta_{ank}}$ ) is needed. In reference [16], we previously calculated the stiffness variation of ankle joint based on the reference [18]. It is shown in Fig.7. All details are presented in [16].

cycle in the derived equations, the power requirements of the exoskeleton joints are calculated as given in Fig. 8. Note that the spring stiffness ( $K$ ) used in all mechanisms are taken as 3 kN/m in the simulation. According to the results, 250 Watt power is required for the first motor of the ankle exoskeleton while 10 Watt power is enough for its second motor. The power requirements of the knee and hip exoskeletons are about 100 Watt and 80 Watt, respectively. The DC motors of the exoskeleton joint mechanisms were selected to meet the power requirements.

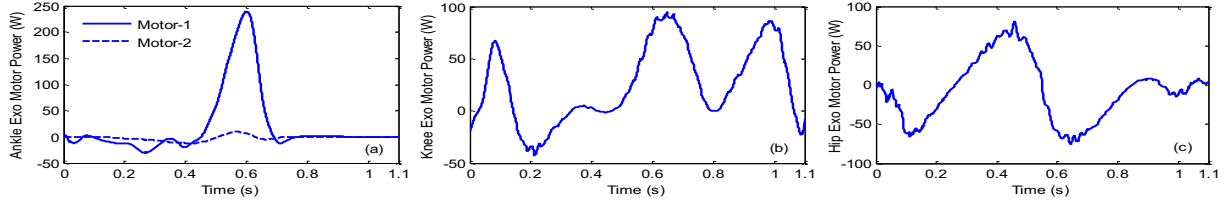


Figure 8. Motor power requirements during gait cycle for (a) ankle, (b) knee and (c) hip joint exoskeletons

#### IV. MECHANICAL DESIGN OF BIOCOMEX

In this section, mechanical design of BioComEx is described in detail. An anthropomorphic architecture with similar kinematics to a human is selected for our design. Thus, it's all ankle, knee and hip joints are active joints. Fig. 9 shows the back and side views of the BioComEx applied on a dummy human model. As can be seen in this figure, the design is constituted of three different exoskeleton robot segments including ankle (right and left), knee (right and left) and hip (right and left) exoskeleton joint mechanisms and a back side connection. While ankle exoskeleton mechanism is embedded into the tibia as a whole, then knee and hip exoskeleton mechanisms are embedded together into the femur. Thus,

it was achieved a compact design. The designs of these exoskeleton joint mechanisms (ankle, knee and hip) are then described in detail. Additionally, the exoskeleton attached to the user via force sensors at the feet, tibia, femur and the chest orthosis parts as shown in Fig.9. In this design, seven force sensors (low cost bending beam load cells) were used for developing modular force feedback control algorithms in future. Those are located in the foot, lower leg, upper leg and back connection of BioComEx as shown in Fig.9. The force sensor in the foot is used to measure the ground reaction force during the contact with the ground of the exoskeleton robot. The other force sensor in the lower leg is used to measure interaction force between the human tibia and the ankle exoskeleton. The force sensor on the upper leg of the



exoskeleton is used to measure the interaction force between the human femur and the upper leg of the exoskeleton. Finally, the load cell in the back is used to measure the interaction force between the back connection and torso of the user. Using the multiple force sensors on different segments of the exoskeleton enables to develop modular force feedback control algorithms in the joints.

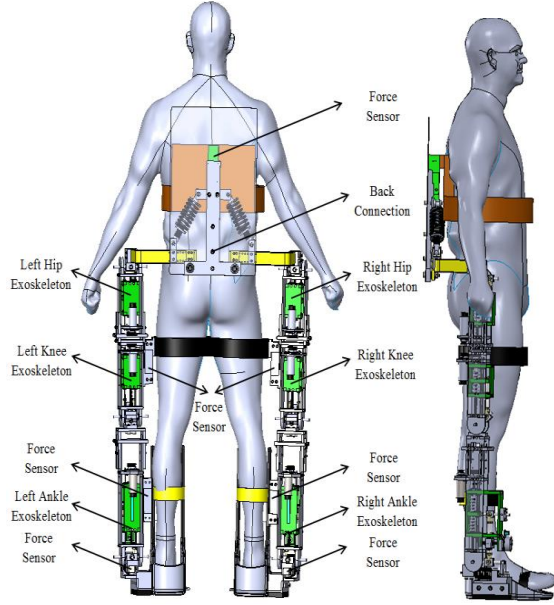


Figure 9. Back and side views of BioComEx

The ankle exoskeleton robot is constituted of ankle foot orthosis, limb length adjustment mechanism and variable stiffness mechanism. It is shown in Fig. 10. The passive ankle foot orthosis (AFO), purchased as ready-made, was used to adapt the variable stiffness ankle

exoskeleton to the user's foot and leg. A limb adjustment mechanism was designed to adjust the limb length of the ankle exoskeleton robot for different persons. Thanks to this mechanism, it is easily adapted to the users with different tibia length. According to [19], the ankle range of motion during the whole gait cycle is approximately  $30^\circ$  (plantar-flexion and dorsi-flexion). The actuator design easily provides the range of motion for the ankle joint during the walking cycles.

As previously mentioned, the single stiffness value is sufficient for the knee joint. Therefore, a series elastic actuator, having a constant stiffness, was designed for the knee joint. The actuator design is shown in Fig. 10. As shown in the figure, motor rotates ball screw via belt and pulley. Thus, the ball screw-nut and series elastic actuator mechanism shown by green color in Fig. 11 moves up and down and it push and pull the force arm vertically, and finally the equilibrium position of the knee exoskeleton changes. Hence, a compliant behavior can be achieved with constant stiffness in the knee joint of the exoskeleton. The range of knee flexion during the one gait cycle is approximately  $70^\circ$  [19]. The design is capable of providing this range of motion for the knee joint during walking cycle.

Similar to knee joint, the single stiffness value is also sufficient for hip joint. Therefore, similar series elastic actuator is designed for hip joint. The design is shown in Fig. 10. The working principle of the hip actuator is similar to the knee actuator. Additionally, there is a upper limb length adjustment mechanism in the hip exoskeleton. Thus, this adjustment mechanism enables to be adapted the hip exoskeleton to the users with different femur lengths. The range of motion of the hip exoskeleton design is approximately  $60^\circ$  ( $20^\circ$  for extension and  $40^\circ$  for flexion). This design meets this required range of motion of the human hip joint for walking [19].

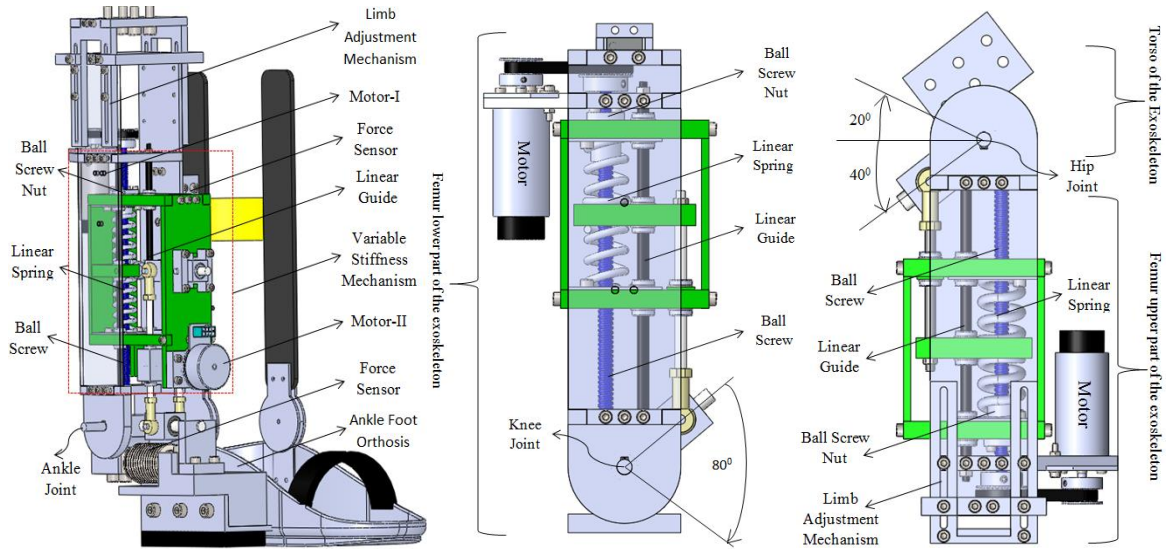


Figure 10. Ankle (left), knee (middle) and hip (right) joint segments of BioComEx

## V. CONCLUSION

In this study, the mechanical design of a new biomimetic compliant lower limb exoskeleton robot (BioComEx) is presented. To mimic biomechanics behavior of the human ankle, a variable stiffness actuator design is used in the ankle of the robot. As one stiffness value is sufficient during gait cycle for the knee and hip joints, a series elastic actuator design, having a single stiffness, is used in the knee and hip joints. In addition, the back connection is designed to grasp the human torso for the purposes of walking assisting and power augmentation. In the design, the ankle joint mechanism is embedded into lower leg, and the knee and hip joint mechanisms are embedded together into the upper leg of the robot and thus, a compact design is achieved. Furthermore, thanks to the limb adjustment mechanism in the tibia and femur parts of the exoskeleton, it is easily adapted to the users with different length. Owing to the separate force sensors attached to all segments of the robot, modular control algorithms can be developed. The next consideration will be producing the whole design and it will be adapted to human body. Later, new control strategies will be developed by using the biomimetic feature of BioComEx.

## ACKNOWLEDGMENT

The authors would like thank to TUBITAK (The Scientific and Technological Research Council of Turkey) for the financial support of a research project numbered with 213M297.

## REFERENCES

- [1] K. Yamamoto, K. Hyodo, M. Ishii and T. Matsuo, "Development of power assisting suit for assisting nurse labor," *JSME International Journal Series C*, vol. 45, no. 3, pp. 703-711, 2002.
- [2] Y. Sankai, "HAL: Hybrid Assistive Limb Based on Cybemics," Book Chapter: Robotics Research; Volume 66 of the series Springer Tracts in Advanced Robotics, pp 25-34, 2011.
- [3] A. B. Zoss, H. Kazerooni and A. Chu, "Biomechanical design of the Berkeley lower extremity exoskeleton (BLEEX)," *IEEE/ASME Transaction on Mechatronics*, vol. 11, no. 2, pp. 128-138, 2006.
- [4] G. Colombo, M. Joerg, R. Schreier and V. Dietz, "Treadmill training of paraplegic patients using a robotic orthosis," *Journal of Rehabilitation Research and Development*, vol. 37, no. 6, pp. 693-700, 2000.
- [5] J. F. Veneman, R. Kruidhof, E. E. G. Hekman, R. Ekkelenkamp, E. H. F. van Asseldonk and H. van der Kooij, "Design and evaluation of the LOPES exoskeleton robot for interactive gait rehabilitation," *IEEE Transactions on Neural Systems and Rehabilitation Engineering*, vol. 15, no. 3, pp. 379-386, 2007.
- [6] S. Freivogel, J. Mehrholz, T. Husak-Sotomayor and D. Schmalohr, "Gait training with the newly developed LokoHelp system is feasible for non-ambulatory patients after stroke, spinal cord and brain injury," A feasible study, *Brain Injury*, vol. 22, no. 7-8, pp. 625-632, 2008.
- [7] G. R. West, "Powered gait orthosis and method of utilizing same," Patent number 6 689 075, 2009.
- [8] S. K. Banala, S. H. Kim, S. K. Agrawal and J. P. Scholz, "Robot assisted gait training with active leg exoskeleton (ALEX)," *IEEE Transaction on Neural Systems and Rehabilitation Engineering*, vol. 17, no. 1, pp. 2-8, 2009.
- [9] O. Unluharsicikli, M. Pietrusinski, B. Weinberg, P. Bonata and C. Mavroidis, "Design and control of a robotic lower extremity exoskeleton for gait rehabilitation," *IEEE/RSJ International Conference on Intelligent Robots and Systems*, pp. 4893-4898, San Francisco, CA, USA, 25-30 Sept. 2011.
- [10] S. Kuitunen, P. Komia and H. Kyrolainen, "Knee and ankle joint stiffness in spring running," *Medicine and Science in Sports and Exercise* vol. 34, pp. 166-173, 2002.
- [11] D. A. Winter and D. G. E. Robertson, "Joint torque and energy patterns in normal gait," *Biological Cybernetics*, vol. 29, pp.137-142, 1978.
- [12] P. Crenna and C. Frigo, "Dynamics of the ankle joints analyzed through moment-angle loops during human walking: gender and age effects," *Human Movement Science*, vol. 30, pp. 1185-1189, 2011.
- [13] K. Shamaei, G. S. Sawicki and A. M. Dollar, "Estimation of quasi-stiffness and propulsive work of the human ankle in the stance phase of walking," *PLoS ONE* 8(3), e59935. doi, 10.1371/Journal.pone.0056635, 2013.
- [14] K. Shamaei, G. S. Sawicki and A. M. Dollar, "Estimation of quasi-stiffness and propulsive work of the human knee in the stance phase of walking," *PLoS ONE* 8(3), e59935. doi, 10.1371/Journal.pone.0059993, 2013.
- [15] K. Shamaei, G. S. Sawicki and A. M. Dollar, "Estimation of quasi-stiffness and propulsive work of the human hip in the stance phase of walking," *PLoS ONE* 8(12), e81841 .doi, 10.1371/Journal.pone.0081841, 2013.
- [16] H. Kizilhan, O. Baser., E. Kilic and N. Ulusoy, "Comparison of Controllable Transmission Ratio Type Variable Stiffness Actuator with Antagonistic and Pre-tension Type Actuators for the Joints Exoskeleton Robots," In *Proceedings of the 12th International Conference on Informatics in Control, Automation and Robotics*, Colmar, Alsace, France, pp. 188-195, 21-23 July 2015.
- [17] G. Bovi, M. Rabuffetti, P. Mazzoleni and M. Ferrarin, "A multiple-task gait analysis approach: kinematic, kinetic and EMG reference data for healthy young and adult subjects," *Gait and Posture*, vol. 33 pp. 6-13, 2010.
- [18] M. A. Holgate, J. K. Hitt, R. D. Bellman, T. G. Sugar and K. W. Hollander, "The SPARK (Spring Ankle with Regenerative kinetics) project: Choosing a DC motor based actuation method," *2nd IEEE RAS & EMBS International Conference on Biomedical Robotics and Bio mechatronics*, Scottsdale, AZ, USA, pp.163-168, 19-22 Oct. 2008.
- [19] J. Perry, "Gait analysis: normal and pathological function," Thorofare, New Jersey: SLACK Incorporated., 1992.